PFC/JA-83-34

# Alcator DCT: Heat Removal and Impurity Control in a Proposed Long Pulse Tokamak

B. Lipschultz, D. B. Montgomery, P. A. Politzer
S. M. Wolfe

Plasma Fusion Center
Massachusetts Institute of Technology
Cambridge, MA 02139

October 1983

This work was supported by the U.S. Department of Energy Contract No. DE-AC02-78ET51013. Reproduction, translation, publication, use and disposal, in whole or in part by or for the United States government is permitted.

# Alcator DCT: Heat Removal and Impurity Control in a Proposed Long Pulse Tokamak.

B. LIPSCHULTZ, D. B. MONTGOMERY, P. A. POLITZER, and S. M. WOLFE,

Plasma Fusion Center, M.I.T.

The most crucial requirement for any heat removal and impurity control system is its performance under steady state loading. The proposed Alcator DCT device at M.I.T. is designed to provide a near term test of long pulse and steady state issues integral to the tokamak program. Anticipated plasma parameters include $\bar{n}_e \sim 10^{14}$ cm$^{-3}$, $T_e \sim$ 3-10 keV, pulse time > 1 minute, plasma currents > 1 Mamp, 1 < ellipticity < 1.6. Superconducting toroidal ($Nb_3Sn$) and poloidal (NbTi) field coils as well as cw RF heating sources allow steady state operation. All day operation using RF current drive is contemplated.

The design parameters most relevant to this discussion are: average wall loading (~ .2Mw/m$^2$), particle pumping rate (~ $10^{21}$ part/sec) and average heat load on the limiter or divertor plates (~ 2-3Mw/m$^2$). We have been studying three configurations which might allow us to obtain these parameters while keeping the impurity level low: 1) pumped limiters, 2) internal poloidal divertors (e.g. ASDEX, PDX, DIVA) and 3) external poloidal divertors (INTOR). Pumped limiters are the simplest of these to implement. On the other hand the physics data base for pumped limiters is small and inadequate for extrapolation to a reactor. There exists a much more extensive physics and engineering

data base concerning divertors. The difference between alternatives 2) and 3) lies in the divertor coil size, location and ease of maintenance. The disadvantages of 2), for a reactor, are that the divertor coil links the TF and cannot be protected properly from neutron damage. While alternative 3) avoids these disadvantages, it requires a large and expensive divertor coil to allow the currents needed. Designs for all three alternatives will be presented and further comparisons made.

The most crucial requirement for any heat removal and impurity control system is its performance under steady state reactor level loading. The proposed Alcator DCT device at M.I.T. will provide a near term test of long pulse and steady state issues integral to the tokamak program. The objectives of the proposed machine are the development of plasma edge, impurity, shape and profile control techniques appropriate to steady state high power operation; the optimization of RF current drive and heating techniques; and the demonstration of an integrated fully superconducting PF and TF magnet system. This paper will give a description of the physical machine and a review of achievable parameters. Three impurity control designs that are contemplated will be described and compared.

## I. Machine description

Alcator DCT is a high field, superconducting tokamak with dimensions and parameters shown in Table I. The TF magnets are constructed with $Nb_3Sn$ cable in conduit, are non-circular in shape, and have a peak field of 10 T at the magnet and 7 T at the plasma major radius. The superconducting PF system uses multi-strand NbTi conductor. The moderate aspect ratio of this device allows an air core transformer providing a flux swing of 35 volt-seconds. This is the only planned tokamak capable of pulse lengths many times the classical magnetic diffusion time. Each toroidal and poloidal field coil has its own separate dewar as well as an overall outer vacuum vessel providing common thermal insulation.

The plasma has a minor radius of 40 cm, elongation up to 1.6, and currents of 1.4 MA. The toroidal field ripple is 2.0% at the plasma edge and .04% on axis. The dee-shaped vacuum vessel has vertical and horizontal dimensions of 155 and 110 cm. This size provides sufficient

room for the internal components accompanying a steady state divertor device. There are are 48 vertical ports and 12 horizontal ports (30 x 70 cm) allowing personnel access to the vessel as well as providing good diagnostic access. These features are illustrated in Figure 1. The engineering for Alcator DCT is described in more detail elsewhere[1].

RF systems consisting of 4 MW at the lower hybrid and 8 MW at the ion cyclotron frequencies are presently on site at M.I.T. Each of these sytems would be upgraded to cw for use on Alcator DCT, with reduction of the available ICRF power to 5 MW.

## II. Achievable plasma parameters

Transport during auxiliary heating has been modelled using two forms for thermal diffusivity derived from PDX "L-mode" neutral beam injection experiments[2], as well as an ohmic scaling to account for "H-mode" confinement.

Transport calculations assuming 9 MW of RF power at the source indicate Alcator DCT can be expected to achieve electron and ion temperatures in the 5 - 10 keV range for average densities of $1 - 2 \times 10^{14} cm^{-3}$. These parameters, together with the available flux swing imply pulse lengths of 1 to 5 minutes, even with the most pessimistic of transport assumptions.

The resulting equilibria exhibit marked finite beta distortions, making possible the study of the evolution and control of high pressure, shaped equilibria for times exceeding the current diffusion time. However, these studies can be performed at or close to the stability boundary only if the more favorable confinement is achieved, or if some additional heating power is supplied.

The available lower hybrid heating can be used to drive current as well as heat the plasma. Predictions using the Fisch-Karney theory

indicate steady state currents of ~ 1 MA could be driven at electron densities > 5 x $10^{13}cm^{-3}$. Studies of the evolution and control of current and pressure profiles with RF current drive will require pulse lengths greater than the plasma L/R time. For the anticipated Alcator DCT parameters this time is of the order of 100 sec. In addition, the demonstration of day-long pulses, which will be required for a tokamak reactor, places severe demands on heat and particle removal and impurity control systems.

## III. Particle and impurity control techniques

A long pulse machine will need particle pumping to allow control over the plasma density. It will also require techniques for minimizing the generation of impurities due to thermal loading and sputtering and for preventing their subsequent entrance into the main plasma. The RF power deposited in Alcator DCT causes a high value of heat (.2 $MW/m^2$) to flow into the plasma edge. This power flux is comparable to values for which large impurity densities are observed during intense auxiliary heating in present day machines. We conclude that on a long time scale a simple limiter can not perform both the tasks of impurity and particle control. Alcator DCT is planned to provide a long pulse test of the two most promising techniques - pumped limiters and poloidal divertors. For the latter option we consider two separate possibilities: an internal poloidal divertor (e.g. PDX[3], ASDEX[4]) and an external poloidal divertor (INTOR[5]). By this we are referring to a divertor produced by coils outside the TF coils. The designs and parameters for the pumped limiter and the two divertor configurations are presented in the following sections.

### Pumped limiter

Much experimental and theoretical research is presently con-

cerned with the subject of pumped limiters. Although small scale experiments[6-9] have produced encouraging results on particle pumping, whether pumped limiters will remove particles efficiently on a large scale tokamak without producing an overabundance of impurities is questionable. While their ease of construction, compared to the extra coils of divertors, causes pumped limiters to be attractive from an engineering viewpoint, we feel it risky to build a long-pulse, high heat flux tokamak with only this option for impurity control.

Our basic design for a pumped limiter is shown in Figure 2a. It is fully toroidal with neutralizer plates located under the limiter at 12 of the 24 bottom vertical ports. Neutrals are therefore created at the entrance of ports where they can be pumped. The limiter has a single leading edge and is flat to allow for plasma discharges of different shapes, sizes and major radii. For the same reasons, the limiter is movable along a major radius. Approximately 10% of all particles entering the scrape-off layer will pass behind the leading edge and strike the neutralizer plate[10]. We estimate that between 10 and 50% of the particles striking the plate will then be pumped. Given that each of the vertical ports has a conductance of $\sim 2 \times 10^4$ 1/sec and that neutral pressures will be similar to present day results ($\sim 10\mu$) we will need $\sim$ 10,000 1/sec of steady state pumping around the torus.

Internal poloidal divertor

The poloidal divertor produced with internal coils is relatively well understood in comparison to the pumped limiter. The exhaust of particles into the region near the pumping ducts is much more efficient than with a pumped limiter. The impurity generation point

is removed from the main plasma edge. Flux multiplication[11] reduces the average energy per ion and impurity-ion friction causes impurities to accumulate in the divertor chamber[12]. Because the prototypical poloidal divertor has toroidal neutralizer plates, the fraction of neutrals created there which are subsequently pumped may be less than a pumped limiter. This problem could be overcome if some part of the exhaust flux were neutralized on plates localized at pump ports. We are studying this idea.

The coil set for this divertor is a triplet similar to that of ASDEX: a main divertor coil and two matching coils carrying an equal but opposite current. These three coils could be superconducting and wound inside the vacuum chamber. The neutralizer plates, covered by coolant-backed tiles, are attached to the main divertor coil. The pair of nulling coils are part of the baffling system defining the divertor chamber (see Figure 2b). The walls of the divertor chamber and parts of the baffles are also covered with cooled tiles to absorb the heat load and erosion caused by the charge exchange flux. The water coolant for these tiles and helium for the superconductors are fed through the supports. The mechanical technique for attaching tiles to the cooled substrate currently being used in TFTR limits the steady state heat load to 10's of watts/$cm^2$. This is insufficient for our application (200-300 $W/cm^2$) and we are currently pursuing alternatives indicated by the INTOR design study[5]: brazing, copper pins and copper wool. One possible configuration is shown in Figure 3. The cooled 'sandwich material' to which the tiles are attached would also be used for bellows cover plates.

External poloidal divertor

The poloidal divertor produced with external coils is not as well understood as the internal poloidal divertor. The only operating device with geometry similar to this class of divertors is the DIII expanded boundary experiment[13] in which divertor coils link the TF coils. The results from the General Atomic and JAERI teams indicate that the expanded boundary exhibits particle pumping and impurity control similar to the PDX and ASDEX divertors. The external poloidal divertor throat is much more 'open' than that of the internal divertor. This could lead to a greater leakage of neutral hydrogen and impurities back to the main plasma. Field lines spread out to a greater extent in the open divertor, allowing easier design of neutralizer plates. When the plasma shape or position is varied, the x-point, and thus the heat flux deposition profile will vary. Our calculations indicate that these variations are less than or of the same order as the $\lambda_E$ variations discussed in Section IV.

We are considering two possible neutralizer plate/baffle configurations for the external divertor. For the first, shown in Figure 2c, the neutralizer plate is mounted directly on the vacuum vessel wall with the baffles below. In the second configuration, shown in Figure 2d, the neutralizer plate and baffle are combined. This is because approximately two thirds of the heat and particle flux contacts the plate near the separatrix. Any neutral created will not have a direct line of sight path back to the main plasma. The fact that the first configuration (Fig. 2c) is not an optimized shape results in higher heat loads, although some of this load will be spread out because of perpendicular transport across the separatrix in the 'divertor chamber'. While this shape is not optimized for heat load, it is easier to con-

struct and support than the second. It is interesting to note that the heat load results for the configuration shown in Figure 2d imply that one should design for the shortest decay length deemed reasonable. This case is somewhat different from the internal poloidal divertor design, which is quite sensitive to the actual value of the decay length.

## IV. Heat deposition calculations

To study the heat deposition profiles, we have chosen the worst case plasma loading, 10 Mwatts at the plasma edge. The energy decay length in the scrape-off layer, $\lambda_E$, which has been scaled from Alcator C results, is 1.2 cm. We have designed the limiter and divertor plates using this value and have calculated the resulting heat deposition if $\lambda_E$ is different by $\pm$ 4 mm.

The heat flux parallel to a field line in the scrape-off layer is calculated on the plasma midplane using the above information. The flux surface geometry is given by the output (Psi(R,z)) of an equilibrium code. The heat flow is then mapped to the divertor plate or limiter surface assuming constant flow on a flux surface. Knowing Psi(R,z) we can calculate the vector components of the magnetic field at the plate, giving the heat deposition. The results for the four different geometries discussed above are shown in Figure 4.

For all cases we find the heat loads and thus the thermally derived impurity sources to be reactor prototypical. Two of the four geometries (4b, 4d) have been optimized for $\lambda_E$ = 1.2 cm, to keep the heat load below 2 MW/m$^2$. The variation of heat loads with changing $\lambda_E$ is manageable.

## V. Edge plasma parameters

A one-dimensional transport code, described in detail elsewhere[14], has been used to model the plasma edge. This calculation includes conductive and convective transport processes as well as neutral and impurity sources (sinks). The field line geometry is adaptable to either magnetically or mechanically limited discharges. For this calculation, as for the heat deposition model, we assume that 10 Mwatts of power is deposited uniformly in the plasma scrape-off region. This power is deposited directly by the RF and/or is transported out of the main plasma. Typical results for the open divertor case are shown in Figure 5. With variation in the plasma density the flux multiplication effect is seen for all divertor configurations. This effect reduces the average energy carried per ion, which also reduces the sputtering at the divertor plate. Since this model predicts the density and temperature in the divertor chamber, we can calculate an impurity accumulation parameter from impurity momentum balance[12]. We find this parameter $[(1/n_i) \times (dn_i/dx)]^{-1}/(L_{div}/3) < 1$ over the complete range in edge conditions.

The parameters for the edge of the main plasma, as opposed to divertor chamber, were roughly similar for all configurations, as the impurity density and power to the edge were kept constant. The edge temperature and electron density ranges were 75 - 100 eV and $.8 - 5 \times 10^{13}$ $cm^{-3}$ respectively. With these values Alcator DCT would enter a sputtering regime typical of that predicted for reactors. Edge and divertor chamber parameters are summarized in Table 1b.

## VI. Summary & conclusions

The three configurations we have considered for the long pulse,

high heat flux Alcator DCT tokamak are a pumped limiter, internal poloidal divertor and external poloidal divertor. For all three we find the heat flux and sputtering regime to be reactor prototypical. The pumped limiter may adequately pump particles if neutralizer plates localized at pump ports prove successful. However, because the surface is at the main plasma edge, similar to simple limiters, we believe pumped limiters are risky with respect to impurity control[15]. Divertors seem more promising for several reasons. The heat is spread out due to the length and spreading of field lines; the impurity generation point is removed from the main plasma edge; pumping is more easily allowed; flux multiplication reduces the average energy per ion, reducing the physical sputtering source; and impurities accumulate in the divertor chamber due to flow of hydrogen ions to the plate. We will therefore include a poloidal divertor, as part of the Alcator DCT design. We feel that with this impurity control option the possibility of achieving long pulses will be greatly enhanced. In addition, we will retain the pumped limiter design as part of the basic machine, providing a comparison of these two particle and impurity control techniques.

Each divertor option presents some advantages. The internal coil design permits a less 'open' divertor chamber. However, the average field line length is greater for the external coil design (Figure 6). This is particularly important for the region $X/\lambda_E < 1$, which contains 2/3 of the edge heat flow. The additional length enhances two divertor chamber effects. The heat load spreads due to perpendicular transport and an impurity generated at the divertor plate must travel further to return to the plasma edge. These effects may balance the openness of the external poloidal divertor. From an engineering viewpoint, we found the two configurations roughly equivalent. At present, we are

pursuing the external poloidal divertor option because of its greater reactor relevance and less understood physics. Techniques for winding a superconducting coil inside the chamber are also being studied should the 'open' divertor fail.

## Acknowledgements

The authors would like to acknowledge the work of the rest of the Alcator DCT design group and Alcator C support staff. In addition, we thank the Argonne reactor study group for their helpful discussions. This work was supported by the U. S. Department of Energy Contract No. DE-AC02-78ET51013.

## References

[1]Alcator DCT Design Group, M.I.T. Plasma Fusion Center Research Report PFC/RR-83-18.

[2]S. Kaye, Transport Analysis Workshop, PPPL, March 1983.

[3]D. Meade, et al., in Controlled Fusion and Plasma Physics (Proc. 9th European Conf., Oxford, 1979) Vol. 1 (1979)91.

[4]M. Keilhacker, et al., 8th International Conference on Plasma Physics and Controlled Nuclear Fusion Research, Brussels, 1980, Vol. II, p. 351.

[5]U. S. FED-INTOR Activity and U. S. Contribution to the International Tokamak Reactor Phase 2-A Workshop.

[6]D. Overskei, Phys. Rev. Letters 46, 177 (1982).

[7]S. Talmadge, et al., J. Nuclear Fusion 22, 1369, (1982).

[8]R. Jacobsen, J. Nuclear Fusion 22, 277 (1982).

[9]P. Mioduszewski, J. Nuclear Materials 111 & 112, 253 (1982).

[10]J. Brooks, private communication.

[11]M. Petravic, et al., Phys. Rev. Letters, 48, 326 (1982).

[12]N. Ohyabu, et al., GA-A16434.

[13]M. A. Mahdavi, et al., GA-A16334.

[14]B. Lipschultz, to be published as an M.I.T. Plasma Fusion Center Report.

[15]E. Marmar, et al., this meeting.

## Figure Captions

Figure 1 Cross-section of Alcator DCT.

Figure 2 Geometries for a) Pumped Limiter, b) Internal Poloidal Divertor, c) External Poloidal Divertor using vacuum vessel wall for mounting neutralizer plate and d) External poloidal divertor shaped to reduce the heat deposition $< 2MW/m^2$.

Figure 3 Tile mounting design.

Figure 4 Heat deposition profiles for the 4 geometries shown in Figure 2. The curves shown are: $\lambda_E = 1.6$ cm (•••); $\lambda_E = 1.2$ cm (——) and $\lambda_E = .8$ cm (---). In cases b) and d) the plates are shaped for $\lambda_E = 1.2$ cm, to force $P_{dep} < 2$ Mwatts/$m^2$ and only one plate out of two is shown.

Figure 5 Typical profiles of $n_e$, $T_e$, $P_{TOT}$, $P_{COND}$, $P_{CONV}$ along a field line for divertor geometry.

Figure 6 Comparison of field line length vs. $\chi/\lambda_E$ on the plasma midplane. The pumped limiter has field line length equal to the asymptotic divertor value for all X.
For $X/\lambda_E = 1$: $\int_0^{X = \lambda_E} P(\psi(\ell))\, d\ell = (2/3)P_{IN}$.

## Table 1a. Physical Characteristics of Alcator DCT

| | |
|---|---|
| Plasma major radius, $R_0$ | 2.0 m |
| Plasma minor radius | 0.40 × 0.56 m |
| Vacuum vessel bore | 1.1 × 1.56 m |
| Toroidal magnetic field ($R = R_0$) | 7.0 T |
| Toroidal field ripple on axis | .04% |
| Maximum field in conductor | 10.0 T |
| TF conductor | $Nb_3Sn$ |
| Poloidal field conductor | NbTi |
| Total flux swing ($R = R_0$) | 35 Wb |
| Plasma Current ($q = 3$) | 1.0 MA |
| Heating | LH 4 MW(cw) |
| | ICRF 5 MW(cw)<br>8 MW (30 sec) |
| Maximum discharge duration (minutes) | 1.5 - 5, w/ohmic |
| | ∞, w/LH current drive |

## Table 1b. Plasma Scrape-off Characteristics

| | |
|---|---|
| $P_{EDGE}$ | 10 Mwatts |
| $\lambda_E$ | 1.2 ± .4 cm |
| $n_E$ | .8 - 5 × $10^{13}cm^{-3}$ |
| $T_e$ | 75 - 150 eV |
| $P_{in}/A_{wall}$ | .19 $\frac{\text{Mwatts}}{m^2}$ |
| $P_{AVE}$ ON DIVERTOR PLATE OR LIMITER | 2 - 3 $\frac{\text{Mwatts}}{m^2}$ |
| CX POWER FROM MAIN PLASMA | 1 Mwatt |
| TOTAL CX & RAD LOSSES IN DIVERTOR | .5 - 6 Mwatts |
| $\lambda_{MFP}$ (IONIZATION OF C) | .5 - 5 cm |

Fig. 1

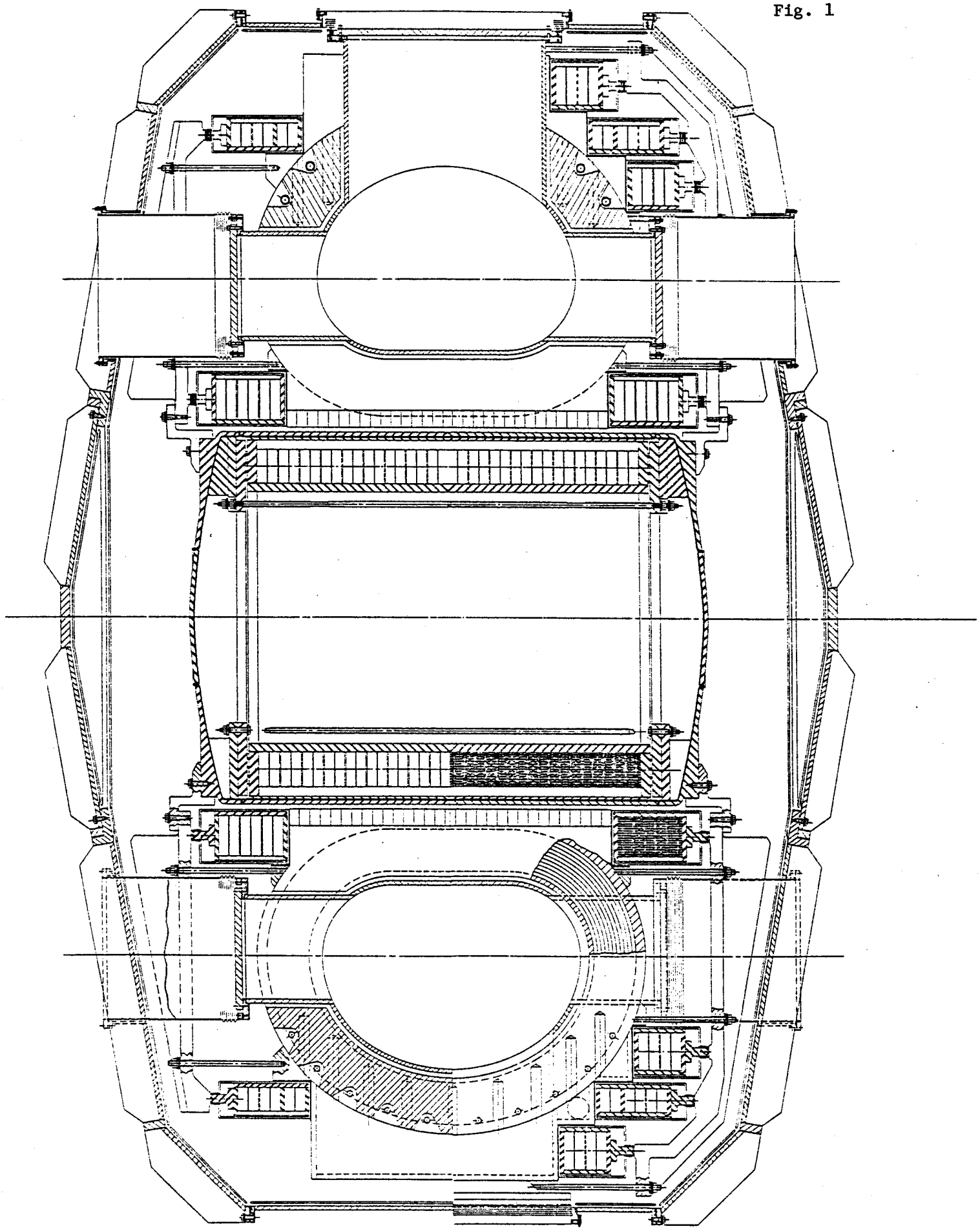

Fig. 2a

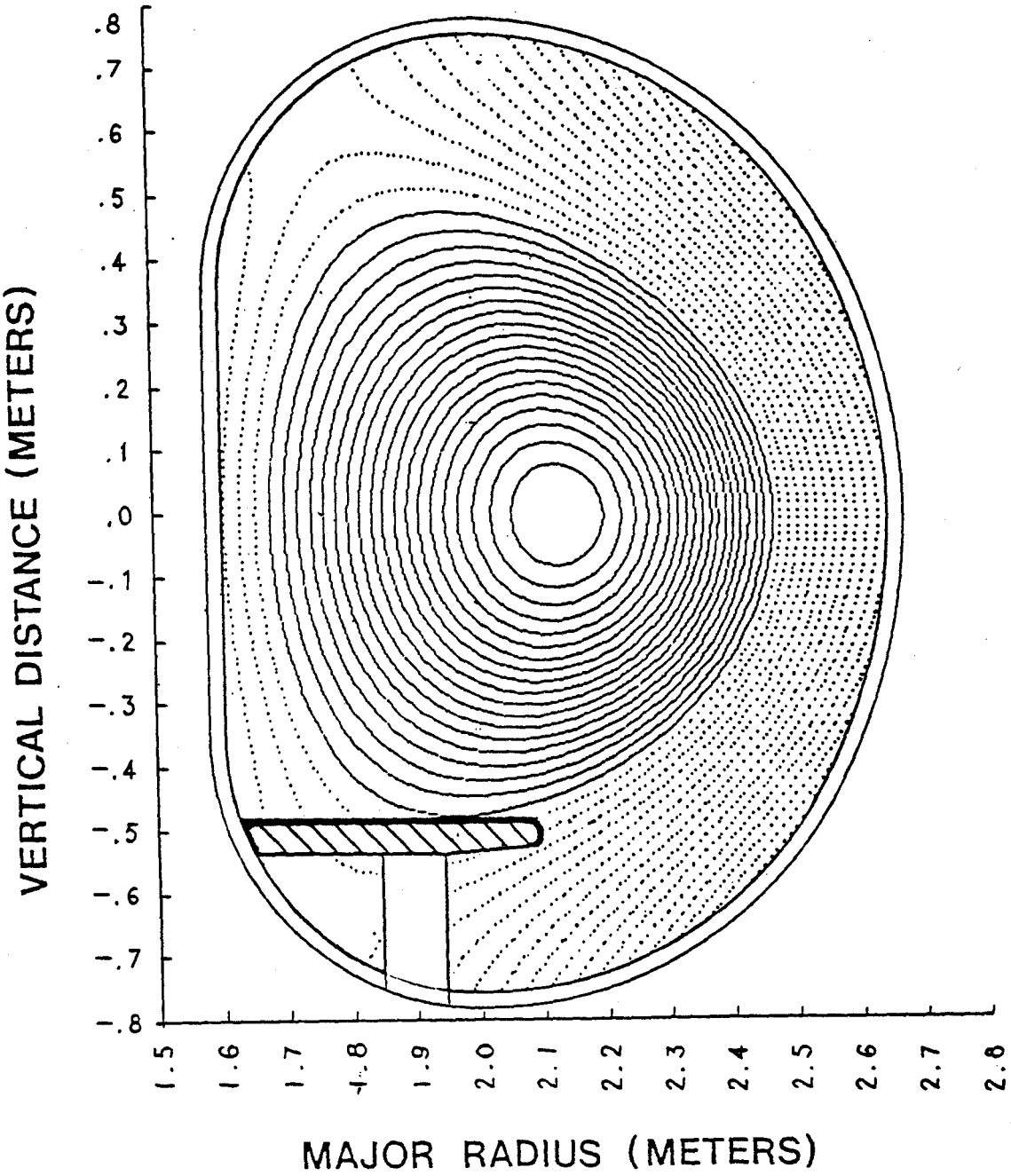
VERTICAL DISTANCE (METERS)
.8
.7
.6
.5
.4
.3
.2
.1
.0
-.1
-.2
-.3
-.4
-.5
-.6
-.7
-.8
1.5
1.6
1.7
1.8
1.9
2.0
2.1
2.2
2.3
2.4
2.5
2.6
2.7
2.8
MAJOR RADIUS (METERS)

Fig. 2b

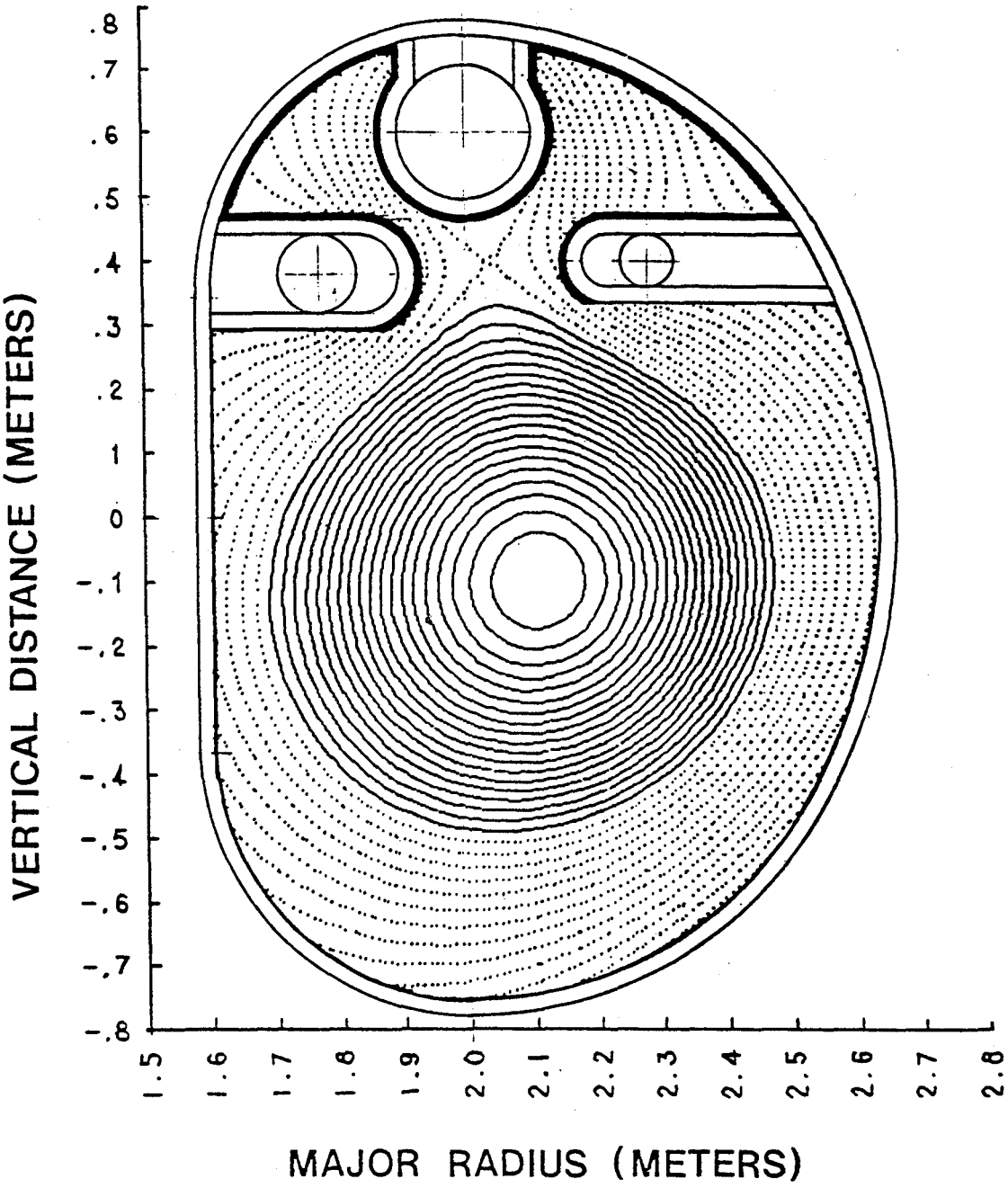
VERTICAL DISTANCE (METERS)
.8
.7
.6
.5
.4
.3
.2
1
0
-.1
-.2
-.3
-.4
-.5
-.6
-.7
-.8
1.5
1.6
1.7
1.8
1.9
2.0
2.1
2.2
2.3
2.4
2.5
2.6
2.7
2.8
MAJOR RADIUS (METERS)

Fig. 2c

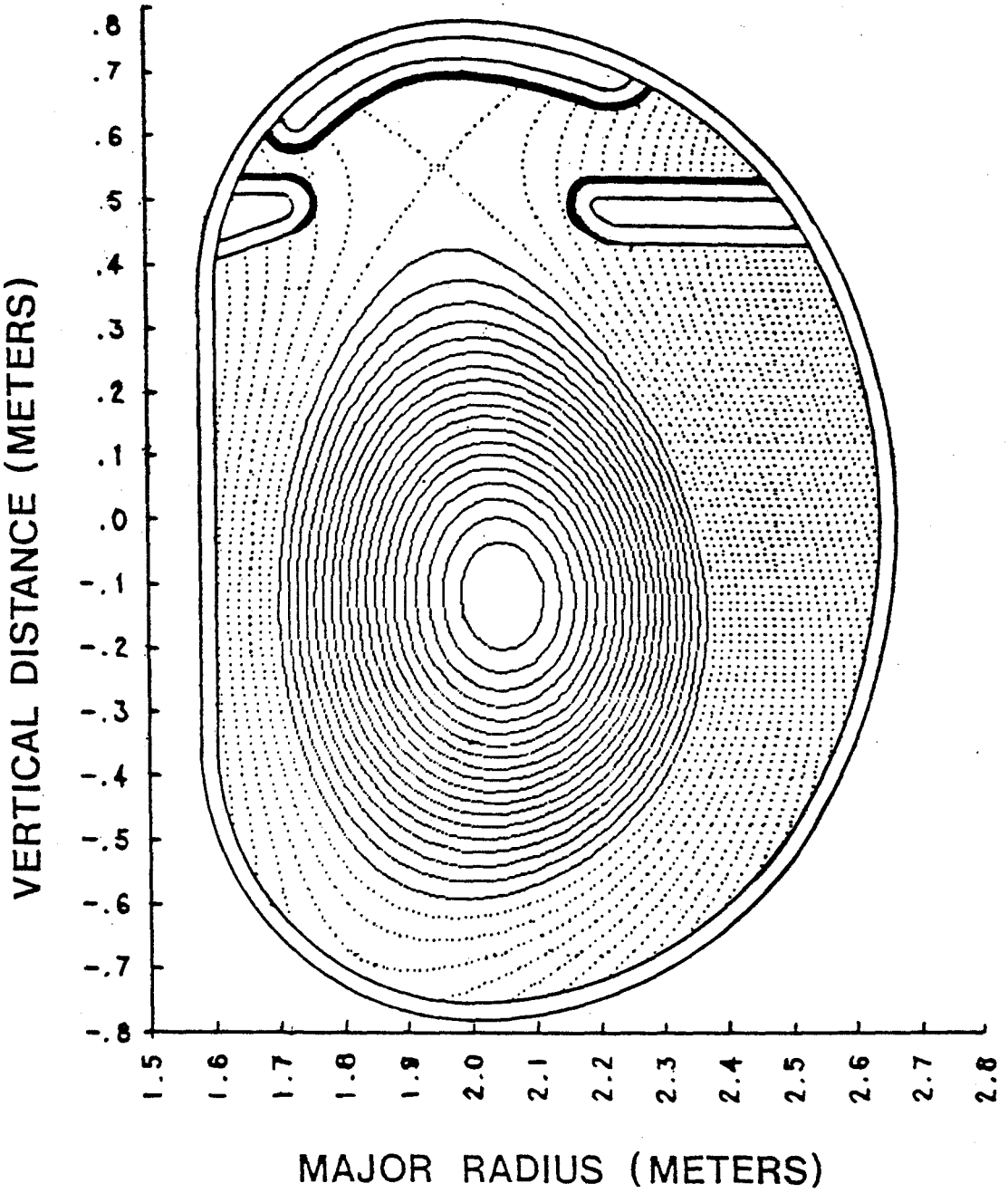
VERTICAL DISTANCE (METERS)
.8
.7
.6
.5
.4
.3
.2
.1
.0
-.1
-.2
-.3
-.4
-.5
-.6
-.7
-.8
1.5
1.6
1.7
1.8
1.9
2.0
2.1
2.2
2.3
2.4
2.5
2.6
2.7
2.8
MAJOR RADIUS (METERS)

Fig. 2d

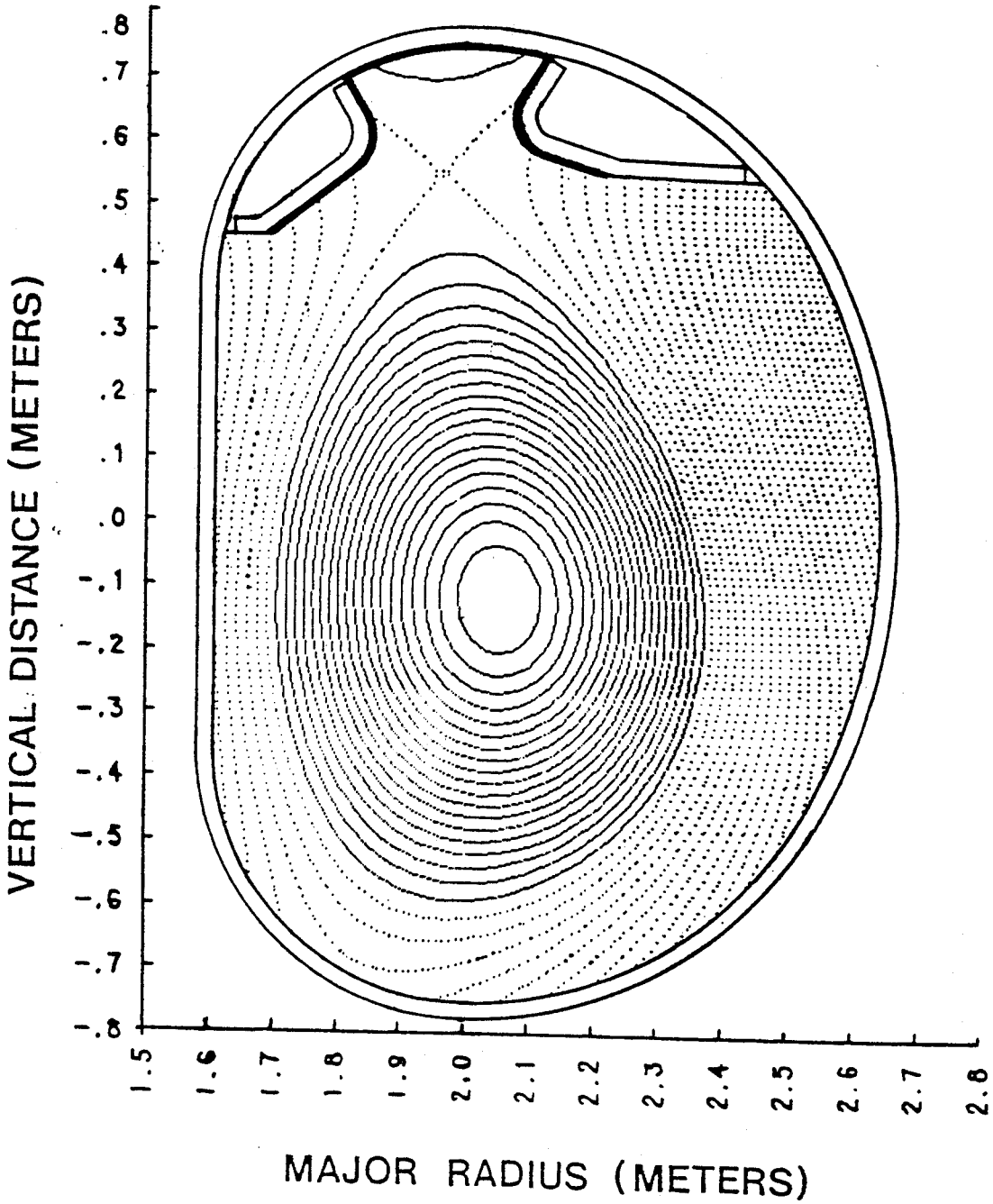
VERTICAL DISTANCE (METERS)
.8
.7
.6
.5
.4
.3
.2
.1
.0
-.1
-.2
-.3
-.4
-.5
-.6
-.7
-.8
1.5
1.6
1.7
1.8
1.9
2.0
2.1
2.2
2.3
2.4
2.5
2.6
2.7
2.8
MAJOR RADIUS (METERS)

Fig. 3

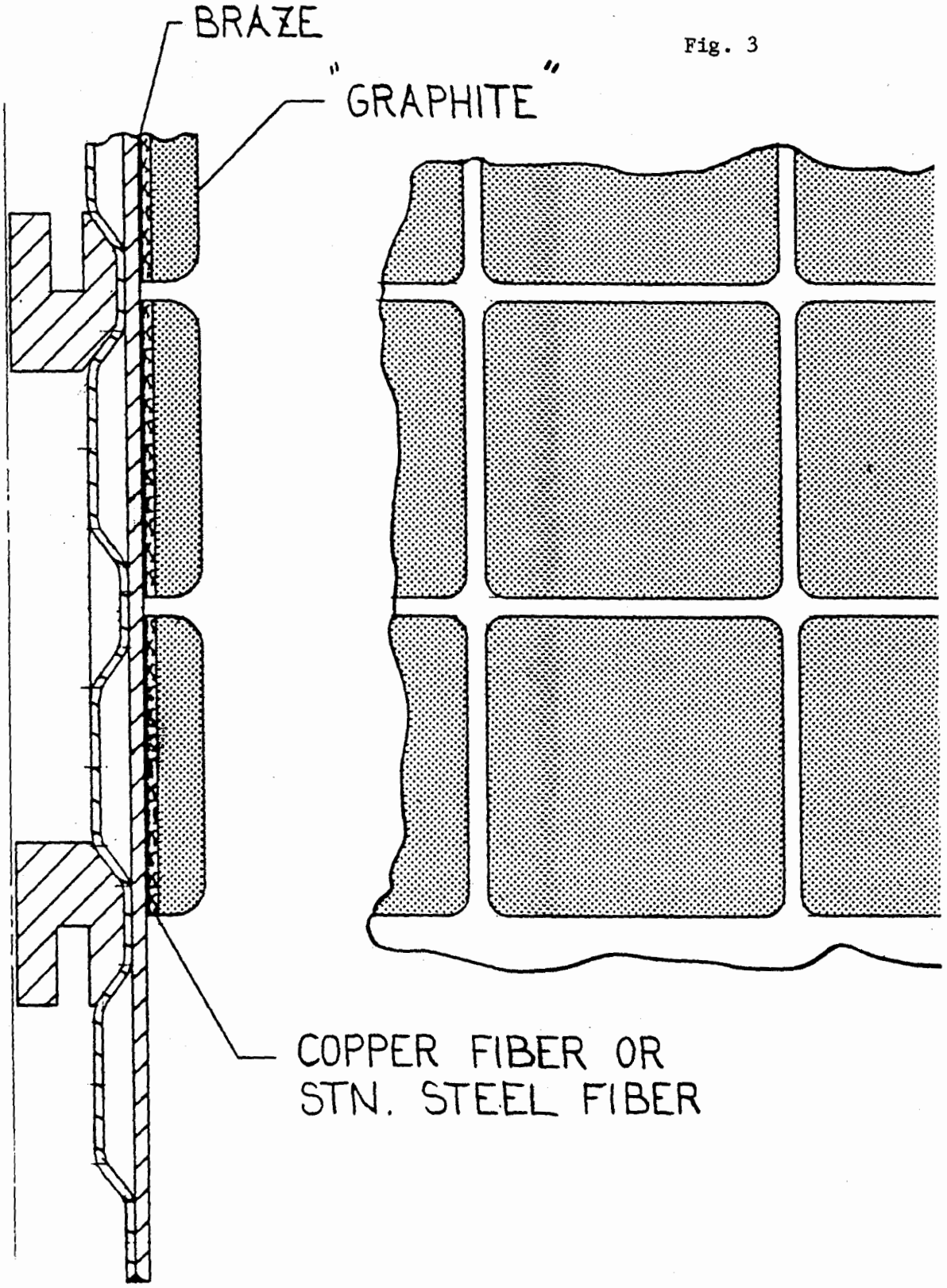

Fig. 4a

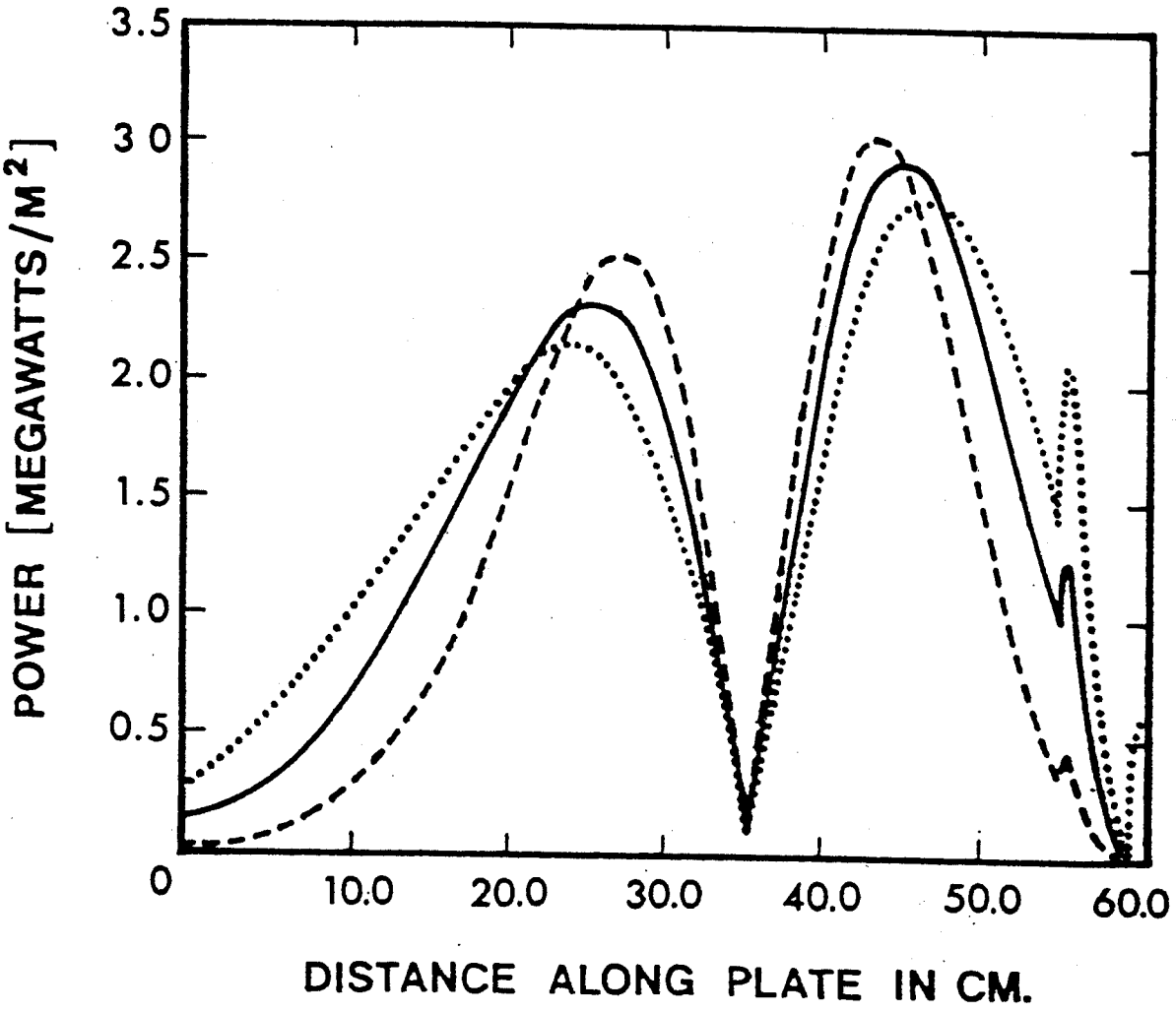
POWER [MEGAWATTS/M²]
3.5
3.0
2.5
2.0
1.5
1.0
0.5
0
10.0
20.0
30.0
40.0
50.0
60.0
DISTANCE ALONG PLATE IN CM.

Fig. 4b

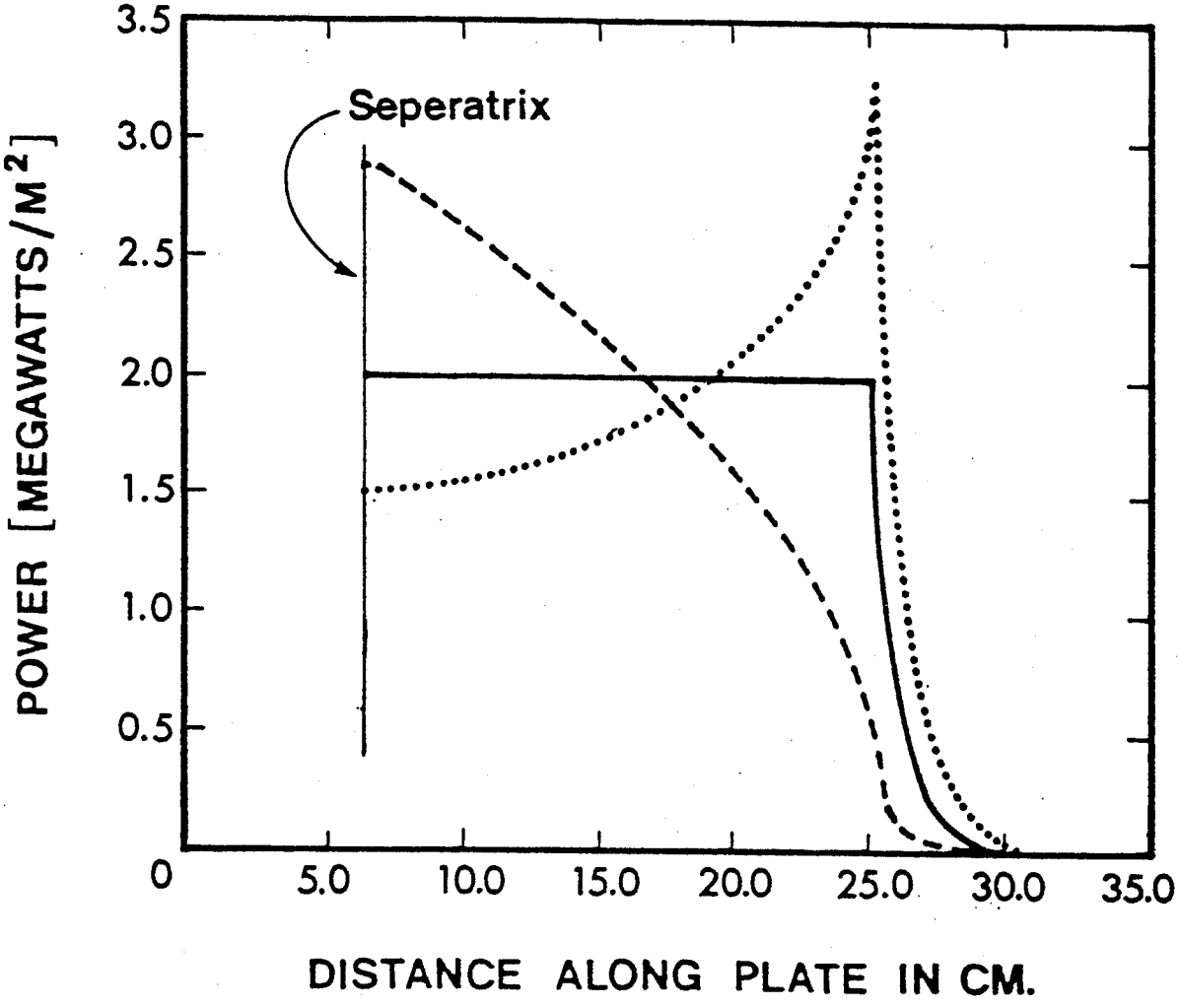
Seperatrix
POWER [MEGAWATTS/M²]
3.5
3.0
2.5
2.0
1.5
1.0
0.5
0
5.0
10.0
15.0
20.0
25.0
30.0
35.0
DISTANCE ALONG PLATE IN CM.

Fig. 4c

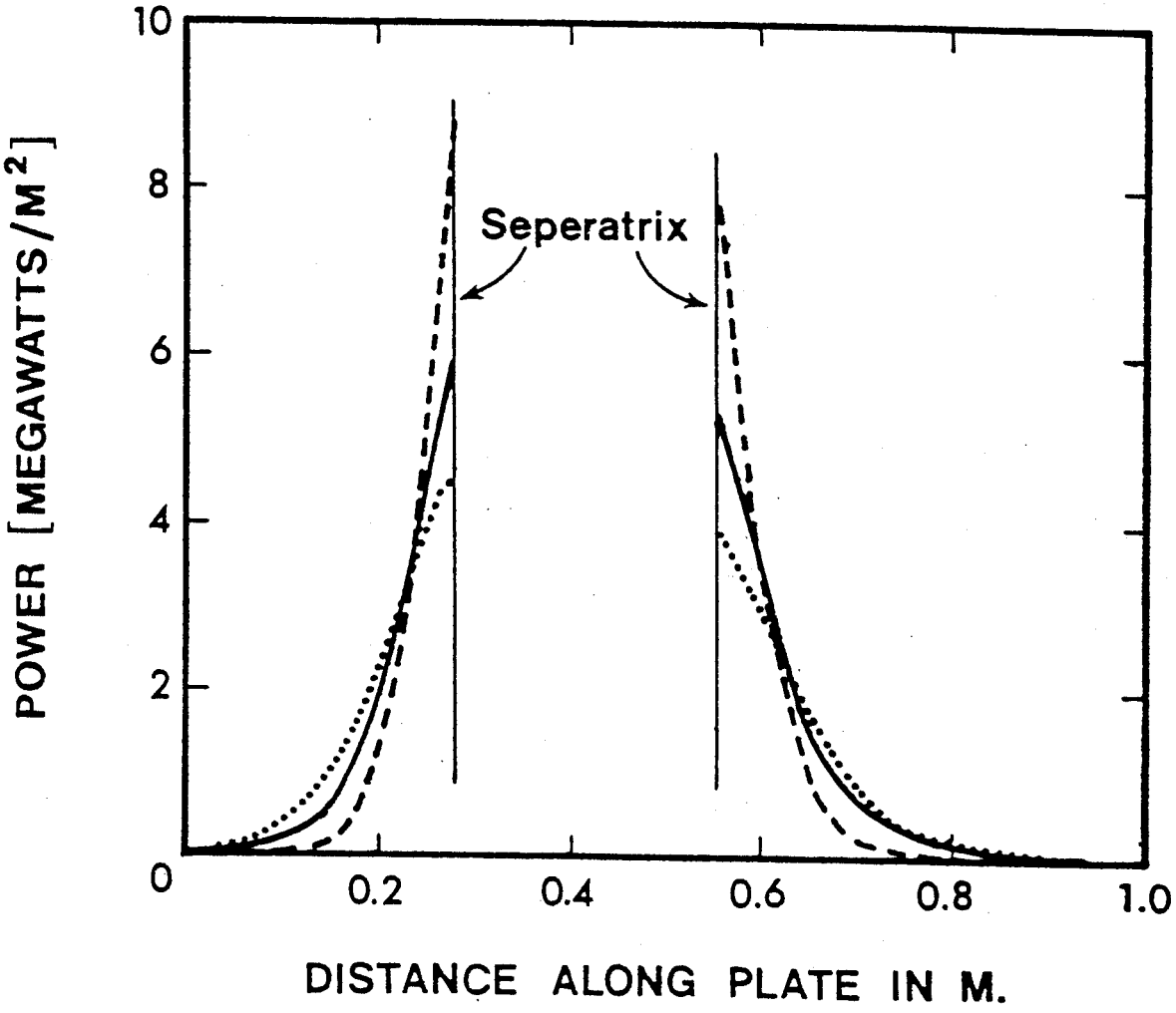
10
8
6
4
2
0
0.2
0.4
0.6
0.8
1.0
Seperatrix
POWER [MEGAWATTS/M$^2$]
DISTANCE ALONG PLATE IN M.

Fig. 4d

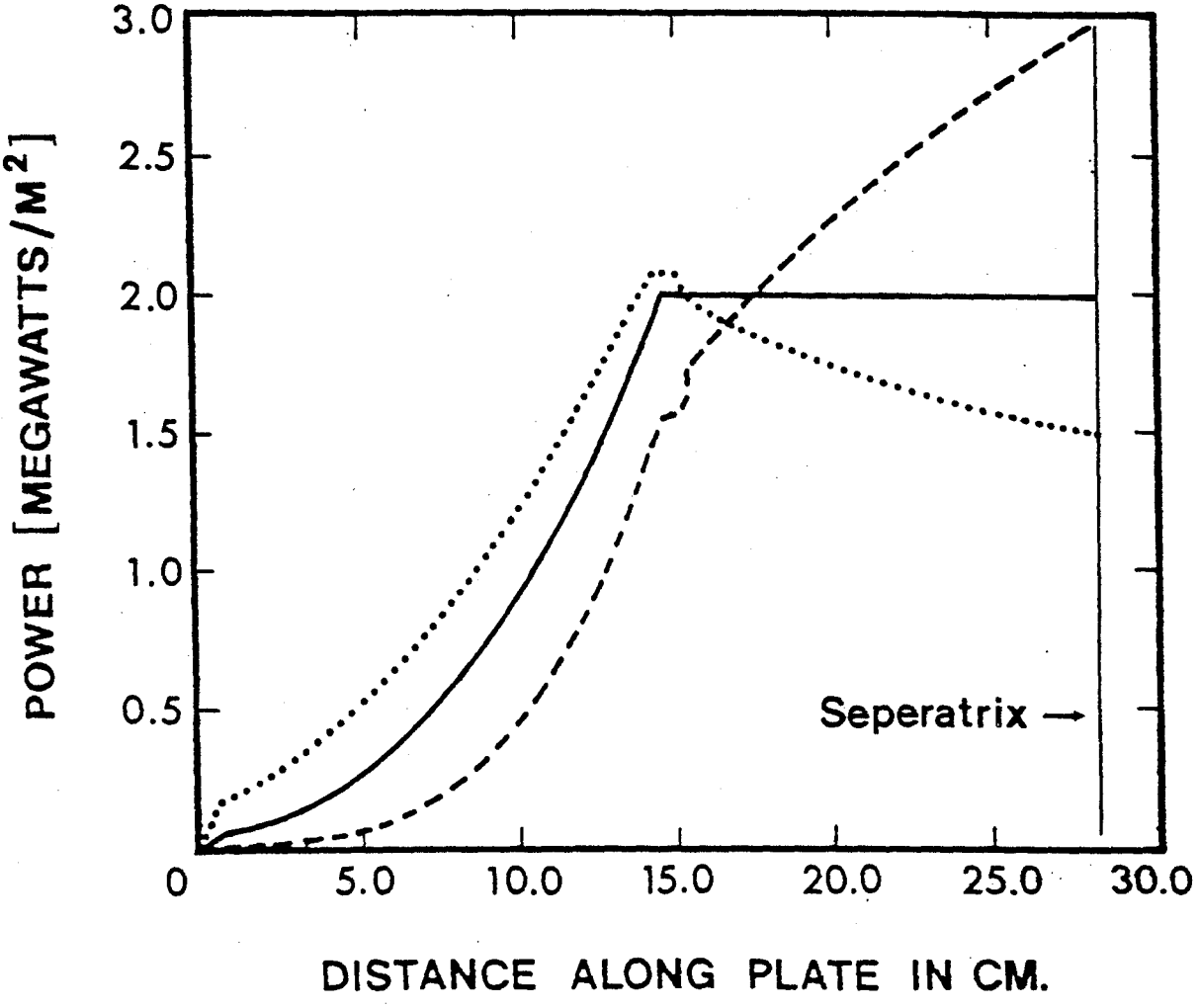
POWER [MEGAWATTS/M²]
3.0
2.5
2.0
1.5
1.0
0.5
0
5.0
10.0
15.0
20.0
25.0
30.0
Seperatrix
DISTANCE ALONG PLATE IN CM.

Fig. 5

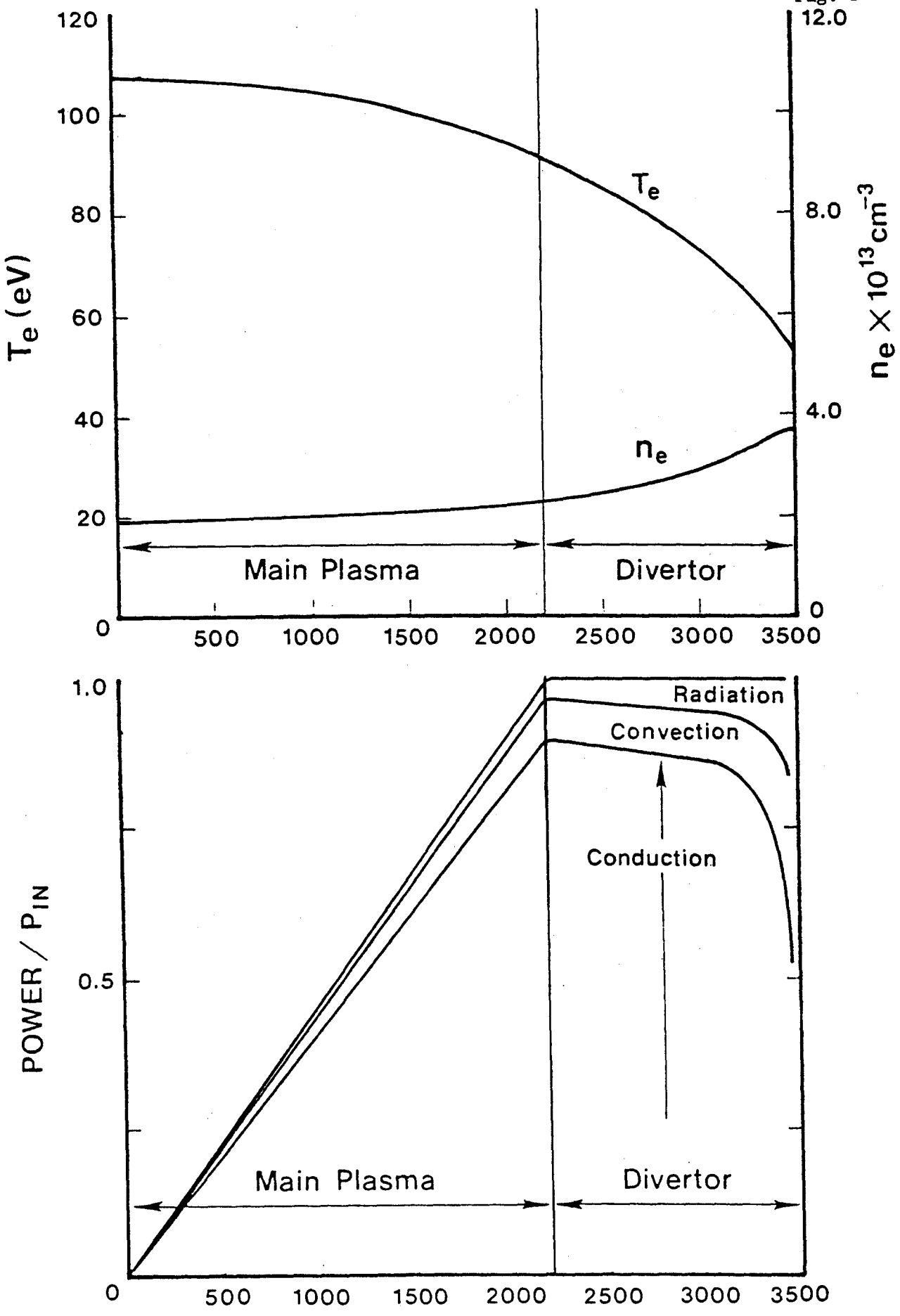
120
100
80
60
40
20
0
$T_e$ (eV)
12.0
8.0
4.0
0
$n_e \times 10^{13} cm^{-3}$
$T_e$
$n_e$
Main Plasma
Divertor
500
1000
1500
2000
2500
3000
3500
1.0
0.5
0
POWER / $P_{IN}$
Radiation
Convection
Conduction
Main Plasma
Divertor
500
1000
1500
2000
2500
3000
3500
DISTANCE ALONG FIELD LINE (cm)

Fig. 6

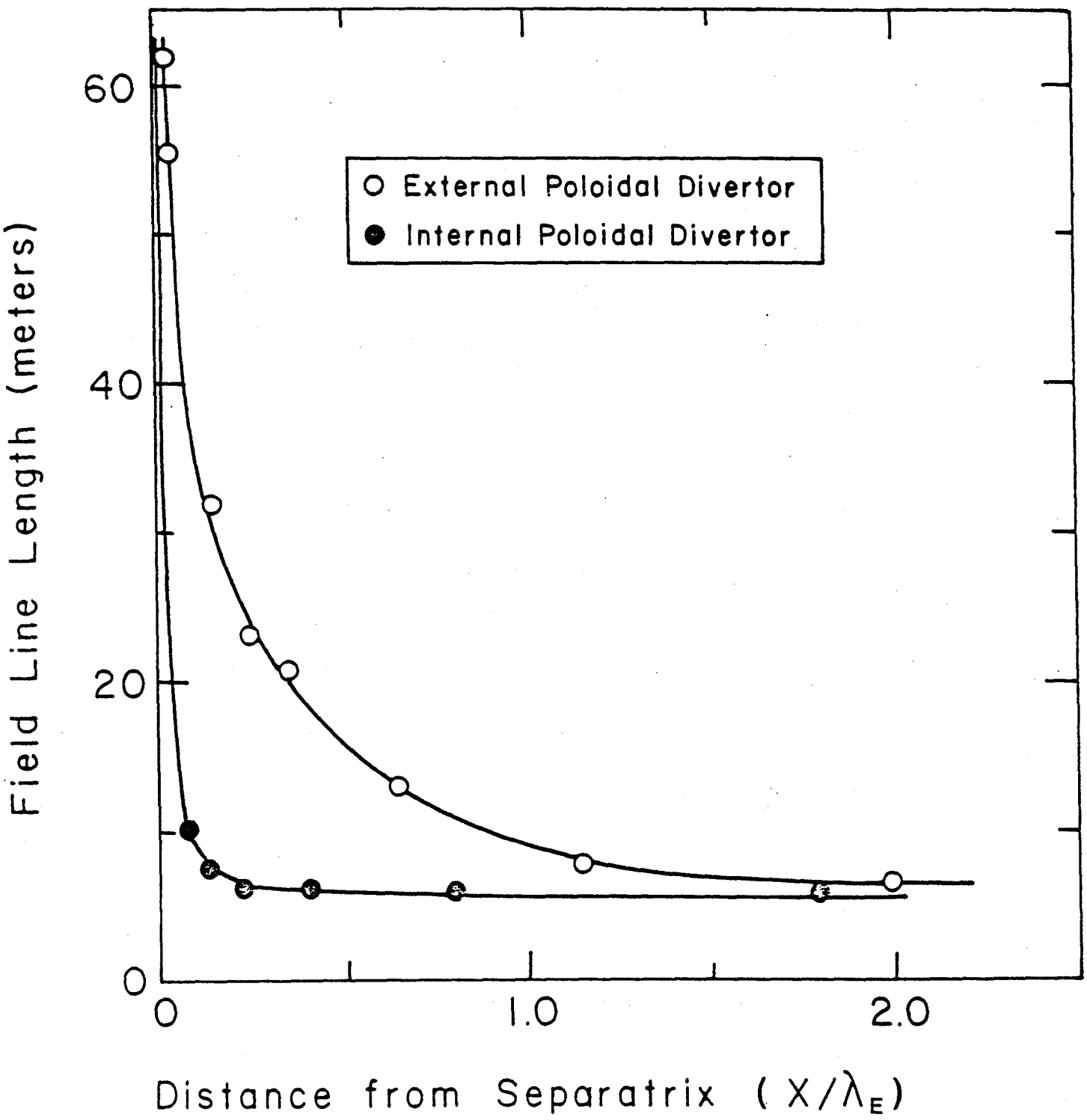
60
40
20
0
0
1.0
2.0
Field Line Length (meters)
Distance from Separatrix ( X/λE)
External Poloidal Divertor
Internal Poloidal Divertor